Research Article

Journal of Environmental Nanotechnology

Enhanced Mechanical and Tribological Performance of Casuarina Fiber-reinforced Epoxy Composites Using ZnO and ZrO_2 Nanoparticles

S. Purushottam Barve[1], Vijayakumar Sivasundar[2], M. Naga Swapna Sri[3], P. Satishkumar[4], N. D. Raja[5], C. Krishnaraj[4], Barun Haldar[6] and S. Mayakannan[4,7*]

[1]Department of Mechanical Engineering, Yeshwantrao Chavan College of Engineering, Nagpur, MH, India
[2]Department of Mechanical Engineering, Saveetha School of Engineering, Saveetha University, Chennai, TN, India
[3]Department of Mechanical Engineering, Prasad V Potluri Siddhartha Institute of Technology, Vijayawada, AP, India
[4]Department of mechanical Engineering, Rathinam Technical Campus, Coimbatore, TN, India
[5]Department of Electronics and Communication Engineering, Sri Venkateshwara College of Engineering, Bengaluru, KA, India
[6]Department of Industrial Engineering, College of Engineering, Imam Mohammad Ibn Saud Islamic University, Riyadh, Saudi Arabia
[7]Department of Mechanical Engineering, Saveetha School of Engineering, Saveetha Institute of Medical and Technical Sciences, Chennai, TN, India

Received: 03.09.2025 Accepted: 29.09.2025 Published: 30.09.2025

*kannanarchieves@gmail.com

ABSTRACT

Natural fiber composites are increasingly explored as eco-friendly and lightweight alternatives to synthetic materials, though their limited mechanical and tribological performance hinders industrial use. In this work, epoxy composites reinforced with casuarina fiber were fabricated and modified with ZnO and ZrO_2 nanoparticles to enhance their properties. Four composites, S1 (epoxy/casuarina fiber), S2 (epoxy/casuarina fiber/ ZrO_2), S3 (epoxy/casuarina fiber/ZnO), and S4 (epoxy/casuarina fiber/ ZrO_2/ZnO), were prepared with a resin-to-fiber ratio of 70:30 and 4 wt% nanoparticle loading. Mechanical (tensile, flexural, impact, hardness) and tribological (wear loss, coefficient of friction) tests revealed that nanoparticle incorporation significantly improved performance, with the ZnO-filled S3 composite showing the best results, achieving a tensile strength of 85 MPa, flexural strength of 125 MPa, impact strength of 7.5 kJ/m², and hardness of 92 Shore D. Wear studies further confirmed minimal wear loss (0.27052 g) and the lowest coefficient of friction (1.91) under 15 N load, 3 m/s velocity, and 1500 m sliding distance. The SEM analysis of worn surfaces supported these findings, displaying severe cracks and debris in the unmodified composites, moderate damage in ZrO_2-filled samples, and smoother surfaces with shallow grooves in ZnO-filled composites, validating their superior load transfer and wear resistance. These results highlight the potential of ZnO and ZrO_2 enhancing the strength and durability of casuarina fiber-reinforced epoxy composites for automotive and structural applications.

Keywords: Natural composite; Casuarina fiber; ZrO_2; ZnO; Mechanical properties; Wear characteristics.

1. INTRODUCTION

The automobile market is expanding due to technological advancements and the affluent lifestyles of people. Concurrently, safety and economic considerations should be significant issues. The expense of automobiles and their components could be decreased by substituting expensive maaterials with more economical alternatives. In the automotive industry, components such as the body, frame, windows, doors, lighting, and driver panel are constructed from composite materials. Polymer composites using agricultural and bio-based fillers, including snake grass, casuarina, and cork, were fabricated in diverse volume fractions. (Parthasarathy *et al.* 2024). Epoxy composites reinforced with *Nelumbo nucifera* fibers and 6–12 wt% ZnO nanoparticles were produced using the hand layup method. The dynamic mechanical properties were improved, indicating superior mechanical performance and environmental resilience (Senniangiri *et al.* 2025). The ideal time of NaOH treatment and the appropriate fiber/filler content resulted in peak mechanical performance (Edlabadkar *et al.* 2025). Alkali treatment improved fiber-matrix adhesion, and hybrid fiber composition diminished environmental impact while fortifying the polymer composite (Harak *et al.* 2024). Polyvinyl alcohol (PVA) composites reinforced with jute and banana fiber were fabricated using 3 wt% ZnO nanofillers. The ZnO exhibits a flexural strength that is 162.59% greater. Decomposition temperatures exhibited a modest rise, corroborating improved mechanical and thermal performance (Tasnim *et al.* 2024).

Polyester bio-composites reinforced with silk waste fibers were produced with a fiber weight fraction of 11–25%, treated with 6% ZnO nanoparticles and 1% citric acid. Bio-composites achieved a maximum flexural strength of 53.47 MPa (Tumusiime *et al.* 2023). The study examined PLA composites reinforced with false banana fibers (5–25% w/w) and ZnO nanoparticles (0–

10% w/w). The optimized hybrid formulation attained a harmonious combination of tensile and flexural performance and water resistance (Dejene and Gudayu, 2025). Epoxy composites reinforced with NaOH-treated jute fiber and chemically modified ZrO_2 nanoparticles were fabricated. Tensile, flexural, and impact strengths improved by 24.5%, 90.8%, and 85.5%, respectively (Biswas *et al.* 2025). Unsaturated polyester composites were reinforced with NaOH-treated jute fibers and vinyl silane-treated ZrO_2 at concentrations ranging from 5% to 45% by weight. Optimal mechanical performance was attained at 35 wt% filler, with SEM tests validating good filler dispersion (Biswas *et al.* 2019).

The ZnO and ZrO_2 nanoparticles improved the impact resistance of natural fiber composites. Hybrid reinforcement enhanced energy absorption and moisture retention, underscoring the significance of optimal nanoparticle loading (Siddiqui *et al.* 2024). The PLA biocomposites reinforced with natural fibers from *Spartium junceum* L. and *Sida hermaphrodita* (SH) were enhanced with ZnO. The SH fibers improved tensile strength by 38.92% (Kovačević *et al.* 2025). Coir fibers were altered with natural fibers and ZnO nanoparticles, and integrated into polymer composites. Tensile strength for latex + SiO_2 fibers increased by 148%, whereas KH550 + ZnO fibers exhibited a 106% enhancement in interfacial strength, a 196% increase in bonding energy, and an 89% rise in interfacial shear strength, hence enhancing fiber–matrix adhesion and overall composite performance (Ru *et al.* 2024).

Kenaf fiber-reinforced biocomposites containing 12.4 wt% ZnO nanoparticles were produced to substitute glass fiber-reinforced sheet molding compound (GF-SMC). Flexural strength improved by 121%, tensile strength by 38%, exhibiting mechanical qualities comparable to that of GF-SMC, with 9% lower energy consumption and a 33% reduction in environmental effect (Wu *et al.* 2020). Woven jute/epoxy composites were augmented with 2–6 wt% ZnO and TiO_2 nanoparticles and evaluated at temperatures ranging from −40 to 27 °C. Nanofillers enhanced tensile, compressive, flexural, and impact strength, in addition to Young's modulus and damping characteristics. Scanning Electron Microscopy validated the distribution of fillers and the mechanisms of failure (Prasob *et al.* 2018). Jute fibers in polypropylene composites were simultaneously treated using silane coupling agents and zinc oxide nanoparticles. The tensile strength and modulus of single fibers increased by 34.3% and 55.8%, respectively, while the transverse and longitudinal tensile strengths of the composite improved by 19.2% and 46.5%, thereby boosting mechanical and interfacial performance (Yang *et al.* 2024). Natural fiber composites using palmyra and sisal fibers inside a natural rubber matrix were augmented with ZnO and ZrO_2. The ZrO_2 composites demonstrated enhanced microstructural performance evaluations (Sampathkumar *et al.* 2024).

Flax/PLA composites underwent treatment with mercerization, stearic acid, and zinc oxide nanoparticles. The combination of mercerization and stearic acid enhanced tensile and bending strengths by 12% and 20%, respectively, while ZnO nanoparticles increased stiffness by 31–58%, albeit with a slight reduction in strength due to PLA degradation at elevated temperatures, making it suitable for applications requiring improved flexural properties and regulated environmental durability (Sbardella *et al.* 2021). Jute/unsaturated polyester composites underwent mercerization treatment and were reinforced with ZnO nanoparticles. The addition of 0.25% ZnO increased tensile strength to 23 MPa, whereas hybrid fluorocarbon (HFC) treatment elevated flexural strength from 46 MPa to 54 MPa, indicating superior mechanical performance (Zaman *et al.* 2022). Eco-friendly unsaturated polyester resin (UPR) composites were reinforced with treated and untreated leather, cow hair, and chicken feather fibers at 2–15 wt%, and improved with ZnO nanoparticles. The optimal 5 wt% mixed fiber with ZnO filler had the highest bending modulus (4400 N/mm²), bending strength (68.91 N/mm^2), tensile modulus (1788.74 N/mm^2), and tensile strength (34.95 N/mm^2), as confirmed by SEM and FTIR analyses (Ali *et al.* 2024).

As per literatutre, no prior research has been reported on the development of natural composites using casuarina fiber reinforced with dual nanofillers such as ZrO_2 and ZnO. This research introduces the fabrication of natural composites from casuarina fiber, aimed at improving their strength by the use of nano-fillers for industrial applications, especially in the automotive industry. The research primarily examines the mechanical and wear characteristics of composites reinforced with ZrO_2 and ZnO nanoparticles. This study is important because of natural composites, despite being lightweight and eco-friendly, frequently do not match the performance of traditional materials.

2. MATERIALS AND METHODS

2.1 Materials

Epoxy (LY556) and hardener (HY951) were procured from Kovai Seenu and Company in Coimbatore, Tamil Nadu, India. ZrO_2 and ZnO nanoparticles were procured from Matrics Enterprises, Nagercoil. Tamil Nadu, India. Fibers were collected from various places in Coimbatore district, Tamilnadu.

2.2 Fiber Preparation

Casuarina fibers are often harvested from the stems or bark of fully grown casuarina trees. Healthy, disease-free plant material was collected and cut into segments measuring around 10 cm. Chemical retting was employed and the fibers were neutralized with a dilute acetic acid solution to eliminate residual alkalinity

(Hossain *et al.* 2023). Clean fibers were dried in the sun until they attained a stable weight to avoid brittleness. Fibers were then chopped into 5 cm length. The fibers were subjected to surface treatments such as alkali (mercerization) treatment to improve mechanical strength and interfacial adhesion in composites. Table 1 shows the physical properties of casuarina fibers.

Table 1. Physical characteristics of casuarina fiber

Properties	Values
Density (g/cm^3)	1.2-1.4
Fiber diameter (*m*m)	100-250
Cellulose (%)	55-65
Fiber length (mm)	20-40
Hemicelluloses (%)	15-25
Lignin (%)	10-20
Tensile strength (MPa)	250-550
Young's modulus (GPa)	5-15

2.3 Preparation of Composites

The composites were fabricated by the hand lay-up method, incorporating fibers for reinforcement and nanoparticles as fillers.

Table 2. Characteristics of ZnO and ZrO_2 nanoparticles

Properties	ZrO_2	ZnO
Purity (%)	>99	>99.5
Density (g/cm^3)	5.61	5.68-6.1
Form	Powder	Powder
Melting point (°C)	1975	2715
Average particle size (nm)	20-200	20-100
Hardness (HV)	4.5	5-6
Shape	Spherical	Spherical

Table 2 shows the characteristics of the nanoparticles employed in this investigation. Fig. 1 illustrates the fabrication process of nanocomposites. Table 3 shows the composition of different composites (S1, S2, S3 and S4) used in the study. The composites were produced in molds measuring 270 × 210 × 3 mm, employing a release agent to prevent material adherence. Epoxy resin and hardener were combined in a 10:1 ratio with continuous agitation until a homogenous mixture was achieved, after which nanoparticles were added at specified weight fractions and properly dispersed to ensure homogeneity. The mold surface, initially treated with a releasing agent, was subsequently coated with the nanoparticle-reinforced epoxy resin mixture. Dried fibers were thereafter dispersed randomly within the mold and saturated with the resin mixture utilizing brushes and rollers to remove trapped air and ensure adequate wetting. The process continued until the desired fiber-resin combination was achieved. The mold was thereafter sealed and exposed to a compressive force of 25 kg to facilitate consolidation and uniform curing. Upon curing, the laminates were meticulously extracted from the mold and cured at ambient temperature for 24 hours prior to being sectioned into standard specimens for mechanical and morphological analysis.

Table 3. Composition of fiber, filler and epoxy matrix

Composites	Casuarina fiber (wt%)	ZnO (wt%)	ZrO_2 (wt%)	Epoxy (wt%)
S1	30	0	0	70
S2	30	0	4	66
S3	30	4	0	66
S4	30	2	2	66

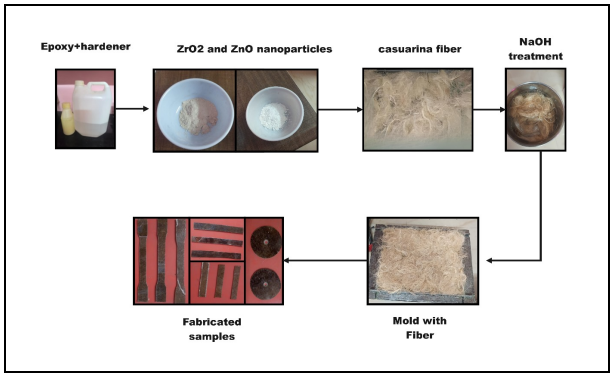


Fig. 1: Fabrication process of the composite

2.4 Experimentation

The strength of the composite was assessed using a universal testing machine (Fig. 2). Tensile strength was assessed in accordance with ASTM D3039 using an INSTRON universal testing machine, at a crosshead speed of 2 mm/min with a maximum load of 5 kN. Using the same equipment, the flexural strength was assessed according to ASTM D7264. As per ASTM D256, the impact strength was determined with the use of an Izod impact tester. A durometer was used to measure the shore D hardness in compliance with ASTM D2240. For each parameter, five measurements were taken, and the average value was calculated for analysis. The wear characteristics of composites were examined according to ASTM G99 employing the pin-on-disc test method.

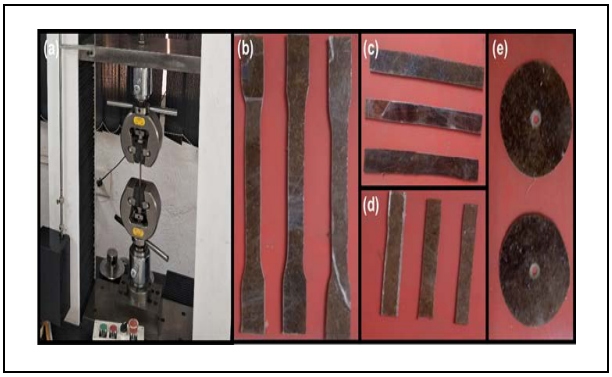


Fig. 2: (a) Universal testing machine; specimen of (b) tensile, (c) flexural, (d) impact and (e) wear tests

Three distinct categories of process parameters were employed namely, load of 10, 15, and 20 N; sliding distance of 1000, 1500, and 2000 m; sliding velocity of 2, 3, and 4 m/s.

3. RESULTS AND DISCUSSION

3.1 Tensile Strength

Fig. 3 illustrates the tensile strength of the casuarina fiber/ZrO_2/ZnO composite. Sample S1 demonstrated minimum tensile strength (75 MPa), whereas, S2, S3, and S4 composites demonstrated superior strengths relative to S1. This is ascribed to the influence of nanoparticle incorporation in S2, S3, and S4 composites. The nanoparticles facilitated the filling of gaps between the fiber and resin, hence enhancing load transfer. Consequently, the lack of reinforcement from nanoparticles in the S1 composite resulted in diminished strength of the material. During testing, the S1 composite sustained significant damage due to insufficient reinforcement and inadequate load transmission. The S3 composite demonstrated superior tensile strength (85 MPa) in comparison to the S2 composite (82 MPa). The S3 composite contained 4 wt% ZnO nanoparticles, while the S2 composite comprised 4 wt% ZrO_2 nanoparticles. The intrinsic properties of nanoparticles resulted in varying strength values. The composites displayed varying strength values due to the inherent features of the ZnO and ZrO_2 nanoparticles, including their chemical composition, hardness, and interaction with the resin matrix. However, the results indicated that ZnO particles facilitated greater stress transfer than ZrO_2 particles due to their superior hardness. This led to superior strength of the S3 composite compared to the S2 material. The S4 composite exhibited intermediate value between the S2 and S3 composites due to the hybrid influence of ZrO_2 and ZnO nanoparticles. Composite S3 demonstrated 11.76% greater tensile strength than that of S1. Similarly, Suja *et al.* (2024) reported that epoxy composites reinforced with casuarina fiber at volumetric concentration of 12% fiber displayed a maximum tensile strength of 29.2 MPa.

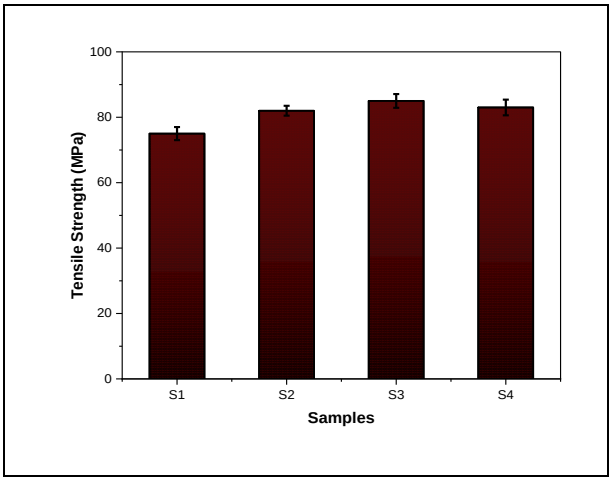


Fig. 3: Tensile strength of casuarina fiber/ZrO_2/ZnO composite samples

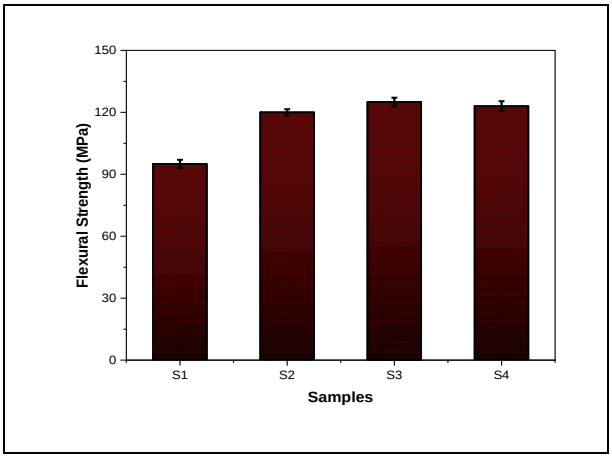


Fig. 4: Flexural strength of casuarina fiber/ZrO_2/ ZnO composite samples

3.2 Flexural Strength

Fig. 4 illustrates the flexural strength of casuarina fiber/ZrO_2/ZnO composites. In contrast to composites S2, S3, and S4, which showed higher flexural strengths, the experimental results showed that S1 had a low flexural strength of 95 MPa. The absence of reinforcing particles resulted in reduced strength of the S1. During the application of bending force, S1 encountered significant surface stress and failed to adequately transfer it due to the absence of nanoparticles. The use of nanoparticles (ZrO_2 and ZnO), contributed to the improvement of flexural strength in S2, S3, and S4 composites. During bending loads, the nanoparticles efficiently facilitated load transfer between the resin and fiber by bridging the interface between the matrix and reinforcement. Consequently, the composites containing nanoparticles exhibited superior strength relative to composites without nano fillers. Moreover, composite S3 demonstrated increased flexural strength (125 MPa) in this study. This was ascribed to the incorporation of ZnO

nanoparticles, which facilitated effective load transfer activities. Moreover, the S2 composite exhibited a flexural strength of 120 MPa, representing a 20.83% increase compared to S1 and a 24% decrease relative to S3. Furthermore, S4 exhibited a moderate flexural strength value compared to S2 and S3 composites, attributable to the hybrid effect demonstrated by the nanoparticles. Likewise, Thandavamoorthy *et al.* (2024) had earlier shown improved flexural strength (64.27 MPa) by the composites of *Prosopis juliflora* fiber with polylactic acid and ZnO nanofillers.

3.3 Impact Strength

Incorporating ZrO_2 and ZnO particles into casuarina fiber-reinforced composites increases their impact strength as seen in Fig. 5. The S1 composite exhibited reduced impact strength (5 kJ/m²). The composites S2, S3, and S4 exhibited improvements in impact strength of 6.5%, 7.5%, and 7%, respectively, when compared to the S1 composite. The addition of nanoparticles established a bonding between the fiber and resin. The composite S3 demonstrated superior impact strength compared to the S2 and S4 composites due to the presence of ZnO particles, which enhanced the energy absorption properties of the composite. The impact strength of the S4 composite was found to be greater than that of the S2 composite and less than that of the S3 composite, attributable to the hybrid effect of nanoparticles. Composite S4 contained 2 wt% ZnO and 2 wt% ZrO_2. The synergistic effect of both particles demonstrated an intermediate strength between the S2 and S3 composites. This study confirms that S3 composite demonstrated the maximum impact strength at 7.5 kJ/m², which is 33.3% more than that of the S1 composite. Similarly, Kumar *et al.* (2023) documented that a maximum impact strength of 28.7% was attained in 6% NaOH-treated kenaf fiber-reinforced epoxy composites (35% fiber) incorporating 3% ZnO nanoparticles, resulting in improved stress transmission and mechanical performance.

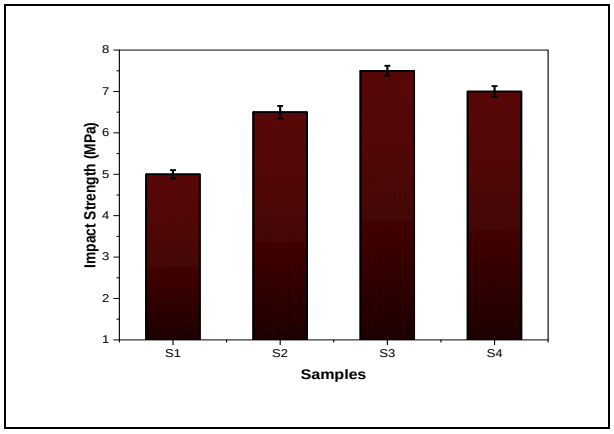


Fig. 5: Impact strength of casuarina fiber/ZrO_2/ZnO composite samples

3.4 Hardness

Fig. 6 illustrates the hardness results of the casuarina fiber/ZrO_2/ ZnO composite. The S1 composite exhibited decreased hardness, but the S2, S3, and S4 composites demonstrated elevated hardness levels. Consequently, the nanoparticles imparted an enhanced reinforcing effect to the S2, S3, and S4 composites, thereby improving the hardness value. The nanoparticles in the S1 composite did not provide adequate reinforcement, resulting in a moderate resistive force at the plunger point. In the case of S2, S3, and S4 composites, the resisting force was enhanced due to the influence of both fibers and nanoparticles. The value of the S3 composite surpassed that of S2 due to the presence of tougher ZnO particles in the S3 composite. The ZnO particles offered adequate resistance to the plunger action, resulting in enhanced hardness for the S3 composite. The S4 composite displayed an intermediate hardness value between the S2 and S3 composites, attributable to the equal proportion of ZrO_2 and ZnO particles with varying hardness levels. The investigation established that the S3 composite demonstrated the highest hardness (92 Shore D), which is 13.04% greater than that of the S1 composite. Shanti *et al.* (2024) likewise had reported a maximum hardness of 63.33% for E-glass fiber-reinforced polyester composites that were fabricated using teak, casuarina fiber, and hybrid fillers, with an optimal loading of 15 wt% and a 1:1 filler distribution.

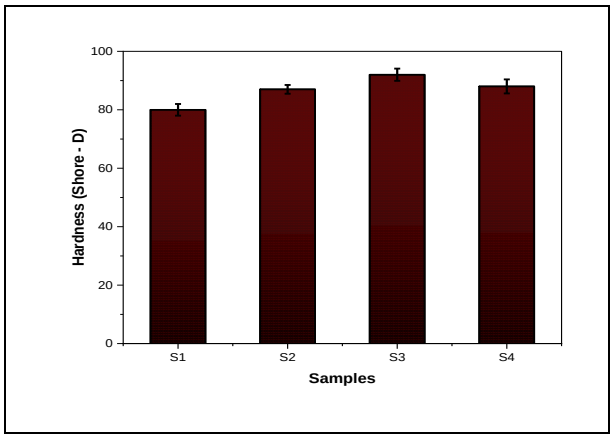


Fig. 6: Hardness of casuarina fiber/ZrO_2/ZnO composite samples

3.5 Analysis of Wear Behaviour

3.5.1 Effect of Applied Load

Fig. 7 illustrates the wear loss of casuarina fiber/ZrO_2/ ZnO material under varying load situations. The report indicated that wear loss was minimized at low loading conditions and maximized under high loading conditions. The counter disc and pin may be under more pressure, which could cause this. Due to the rise in

pressure, heat was generated in the material. This compromised the material's integrity and diminished the adhesion between the matrix and fiber. Wear loss was substantial for S1 composite and was less for the S2, S3, and S4 varieties. The absence of reinforcing particles in the S1 composite resulted in increased wear loss. The reinforcing particles in S2, S3, and S4 composites mitigated significant material degradation during the sliding movement. With a load of 15 N, a sliding velocity of 3m/s, and a sliding distance of 1500 m, S3 composite showed a negligible wear loss of 0.27052 g. When compared to S1 composite under the same wear conditions, composite S3 had a 11.74 % lower wear loss. Similarly, when flax/glass fiber epoxy composites with 0–0.5 wt% ZnO nanofillers were assessed for tribological performance, composites with 0.3 wt% ZnO exhibited diminished wear rates attributed to improved epoxy-fiber adhesion (Meravi and Panchore, 2025).

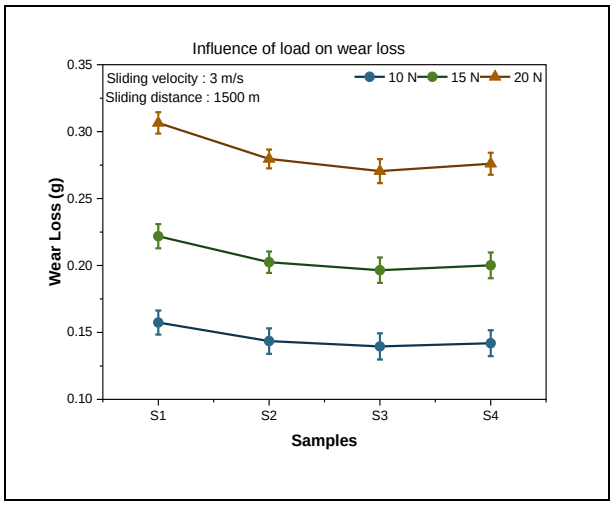


Fig. 7: Impact of applied load on wear loss for casuarina fiber/ZrO_2/ZnO composites

3.5.2 Effect of Sliding Velocity

Fig. 8 illustrates the wear loss of casuarina fiber/ZrO_2/ZnO composite under varying sliding velocity circumstances. The plot shown that increased wear at high velocity and reduced wear at low velocity. As the sliding velocity increases, a greater quantity of frictional heat was generated. This compromised the composite structure and weakened the material. The result was a larger amount of material being extracted during the sliding process. Material breakage and more material loss were caused by the increased shear stress on the composite surface, which was driven by the elevated sliding velocity. The reinforcing action of nanoparticles led to reduced wear losses in the S2, S3, and S4 composites relative to S1. Moreover, the S3 composite exhibited reduced wear loss compared to the S2 composite, attributable to the incorporation of ZnO nanoparticles.

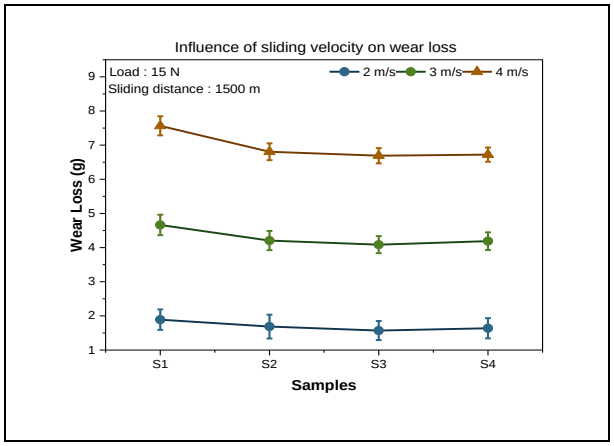


Fig. 8: Impact of sliding velocity on wear loss for casuarina fiber/ZrO_2/ZnO composites

3.5.3 Effect of Sliding Distance

Fig. 9 illustrates the wear loss of casuarina fiber/ZrO_2/ZnO composite under varying sliding distance. The composite experienced significant wear under high sliding distance conditions and minimal wear loss under low sliding distance conditions. When the sliding distance was low, the contact duration between the pin and counter disc was reduced. Likewise, under conditions of extended sliding distance, the contact duration increased, leading to more heat generation in the composite. This resulted in increased wear loss due to the facilitated removal of material under warm conditions. The composite S1 demonstrated increased wear loss attributable to a lack of reinforcement. Additionally, the other composites, S2, S3, and S4 exhibited reduced wear loss attributable to the use of reinforcing particles that effectively limited material removal. Moreover, S3 exhibited the minimal wear loss across all sliding distance circumstances due to the strengthening action of hard ZnO particles.

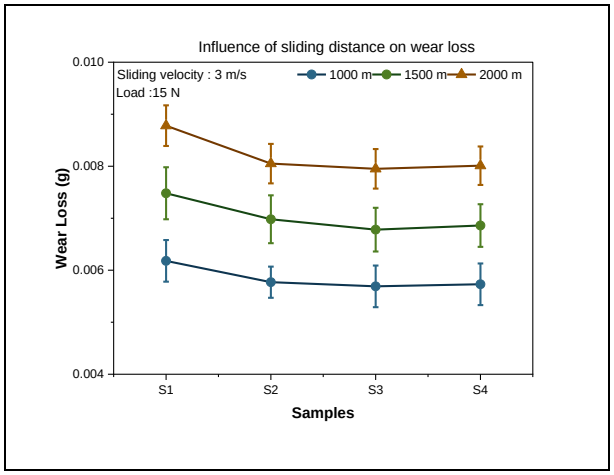


Fig. 9: Impact of sliding distance on wear loss for casuarina fiber/ZrO_2/ZnO composites

3.6 Coefficient of Friction (COF)

3.6.1 Effect of Applied Load

Fig. 10 presents the coefficient of friction report for casuarina fiber/ZrO_2/ZnO composites under varying load circumstances. The results indicated that the composites had a high COF at lower loading levels and a low COF at higher loading conditions. The pin and counter disc were under more pressure, which caused this. The increase in pressure elevated the normal force between the mating surfaces, resulting in a reduction of the COF. In addition, the coefficients of friction for the S1 composite were greater than those of S2, S3, and S4. This suggested that the S1 composite endured significant frictional forces owing to the material's pliable characteristics. The reduced frictional forces acting on the S2, S3, and S4 composites resulted in lower COF values than those of the S1 composite. This was accomplished because to the strengthening influence of nanoparticles incorporated into the composites. Due to the increased load-bearing capacity provided by the ZnO particles included in the S3 composite, it showed the lowest coefficient of friction when compared to the S2 and S4 composites. At 3 m/s, 1500 m/s, and 15 N of load, the S3 composite had the lowest COF value of 1.91, according to this investigation. The COF value of the S1 composite, evaluated under the same processing conditions, is 10.75 % points higher than this number. Jute/flax hybrid composites were augmented with ZnO (1.5%) fillers. Wear experiments demonstrated diminished matrix deformation, decreased COF, and enhanced wear resistance, with artificial neural network (ANN) models precisely forecasting COF and wear as observed by (Demir, 2025).

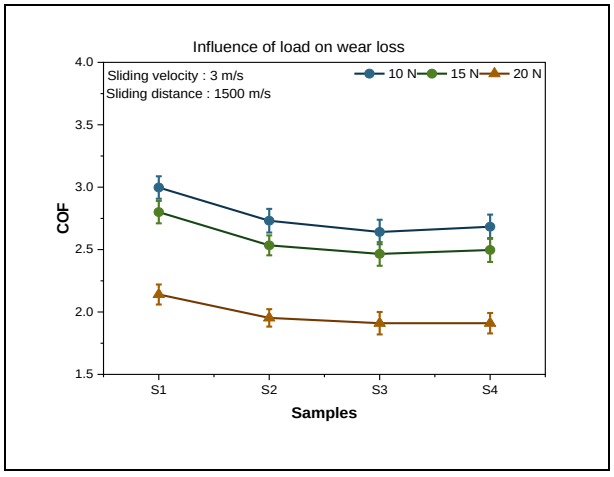


Fig. 10: Impact of applied load on COF for casuarina fiber/ZrO_2/ZnO composites

3.6.2 Effect of Sliding Velocity

Fig. 11 illustrates the coefficient of friction results for casuarina fiber/ZrO_2/ZnO material under varying sliding velocity circumstances. The composites exhibited improved coefficients of friction with increasing sliding velocities. As the sliding velocity increases, the friction between the composite material and the rotating disc also intensified. This resulted in an elevation of the COF value. In addition, the COF values of S1 were greater than those of S2, S3, and S4. This suggested that S1 had increased frictional forces due to the lack of reinforcement. The S3 composite demonstrated a lower coefficient of friction than the S2 composite. This is due the ZnO particles that improve its load-bearing ability and is more effective than the S2 composite, which uses ZrO_2 particles. The S4 composite exhibited a moderate coefficient of friction compared to the S2 and S3 composites due to the hybrid influence of nanoparticles.

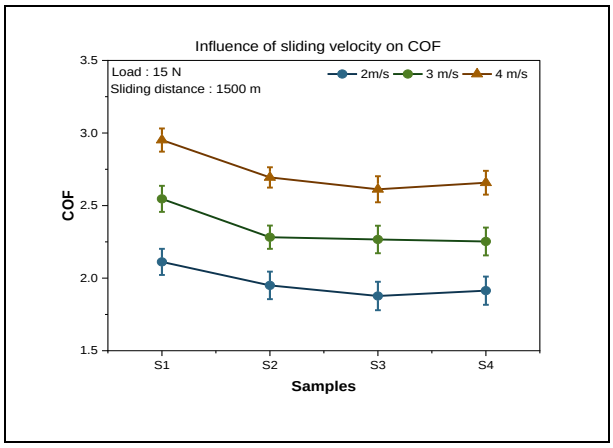


Fig. 11: Impact of sliding velocity on COF for casuarina fiber/ZrO_2/ZnO composites

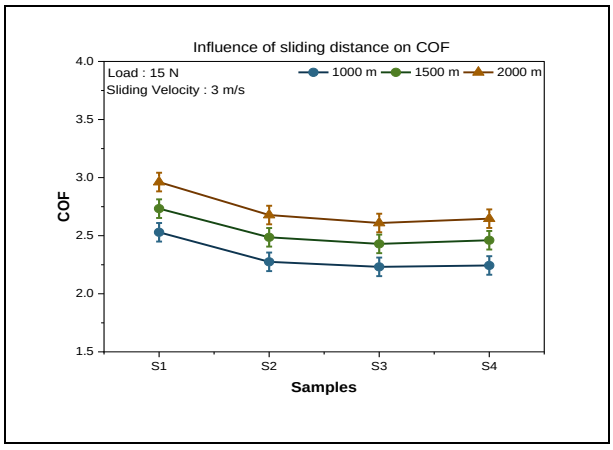


Fig. 12: Impact of sliding distance on COF for casuarina fiber/ZrO_2/ZnO composites

3.6.3 Effect of Sliding Distance

Fig.12 presents the coefficient of friction results for casuarina fiber/ZrO_2/ZnO material under varying sliding distance conditions. All composites demonstrated elevated coefficient of friction values with extended

sliding distance. At higher sliding distances, the contact duration between the sample and the counter disc was prolonged, resulting in increased frictional forces; thus, the COF value increases. There was less frictional force and a low COF value at lower sliding distances because the contact duration was reduced. Moreover, S1 exhibited a high coefficient of friction due to the lack of reinforcement. The composite S3 had the lowest coefficient of friction in this study because the ZnO particles added to it increased its load-bearing ability.

3.7 Morphology of Worn-out Surfaces

Fig. 13 illustrates the worn out surface morphologies of the tested composites. In Fig.13(a), the S1 composite consisting of epoxy reinforced with casuarina fiber, displays severe surface damage characterized by cracks and large debris particles. This indicates poor wear resistance due to the absence of nanoparticle reinforcement. Fig. 13(b) corresponds to the S2 composite, where the incorporation of ZrO_2 nanoparticles resulted in fewer surface cracks and relatively smoother regions, though some furrows and fragmented debris were visible. This suggests improved wear resistance compared to S1 composite. Fig. 13(c) depicts the S3 composite reinforced with ZnO nanoparticles, showing a comparatively smoother surface with shallow grooves and fine depressions. The reduction in severe cracks and wear tracks confirms that the addition of ZnO nanoparticles enhanced the composite's hardness and wear resistance more effectively than the other samples. Al-Lhaibi and Al-Shabander, (2022) reported that when epoxy composites reinforced with wood dust and ZnO nanoparticles exhibited enhanced mechanical performance at appropriate nanoparticle loading. It was validated by SEM analysis confirming effective filler dispersion.

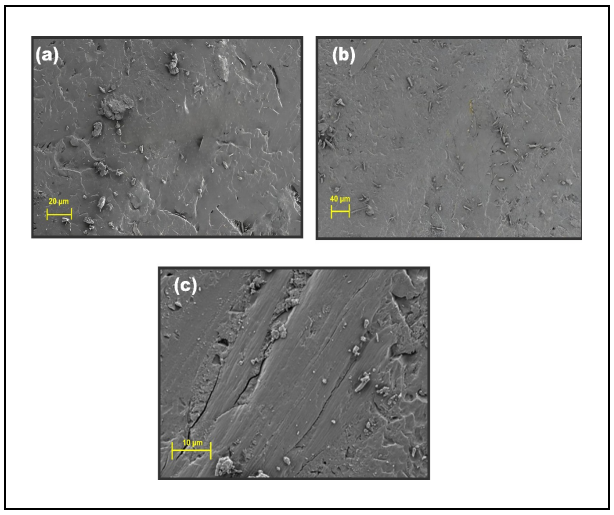


Fig. 13: Micrographs of composites with worn out surfaces (a) S1, (b) S2 and (c) S3

4. CONCLUSION

Casuarina fiber-reinforced composites enhanced with ZrO_2 and ZnO nanoparticles were studied in this experiment. The wear and mechanical performance of composites were subsequently investigated. The subsequent points were derived from the investigation. Due to the reinforcing effect of the nanoparticles, the composite enhanced with ZrO_2 and ZnO particles performed better than the unaltered composite. The S3 composite, which contained ZnO particles and casuarina fiber, had a high tensile strength of 85 MPa. This exceeds the tensile strength of the S1 composite by 11.76%. Additionally, the S3 composite demonstrated an impressive flexural strength of 125 MPa, which can be attributed to the exceptional load transmission capabilities of the ZnO particles. Moreover, S3 demonstrated enhanced impact strength (7.5 kJ/m^2) attributable to the greater energy absorption by the zinc oxide particles and fibers. The Shore D hardness of S3 was 92, which is the highest compared to other specimens. This is 13.04% higher than the S1 composite. At a sliding velocity of 3 m/s, a sliding distance of 1500 m, and a load of 15 N, the wear study showed that the S3 composite had a COF value of 1.91and a minimal wear loss of 0.27052 g.

AUTHOR CONTRIBUTIONS STATEMENT

Conceptualization and Supervision – P. Satishkumar and Barun Haldar. Methodology and Experimental Design – Purushottam S. Barve, and M. Naga Swapna Sri, C. Krishnaraj. Composite Fabrication and Experimental Investigation - Vijayakumar Sivasundar, N. D. Raja, S. Mayakannan. Data Analysis and Interpretation: Purushottam S. Barve, P. Satishkumar and Barun Haldar. Original Draft Preparation: M. Naga Swapna Sri, Vijayakumar Sivasundar. Review and Editing: P. Satishkumar, C. Krishnaraj, S. Mayakannan. Project Administration: S. Mayakannan.

FUNDING

This research received no specific grant from any funding agency in the public, commercial, or not-for-profit sectors.

CONFLICTS OF INTEREST

The authors declare that there is no conflict of interest.

COPYRIGHT

This article is an open-access article distributed under the terms and conditions of the Creative Commons

Attribution (CC BY) license (http://creativecommons.org/licenses/by/4.0/)



REFERENCES

Ali, M. F., Hossain, M. S., Lithi, I. J., Ahmed, S. and Chowdhury, A. M. S., Fabrication and characterization of sustainable composites from animal fibers reinforced unsaturated polyester resin. *Heliyon.,* 10(13), e33441(2024). https://doi.org/10.1016/j.heliyon.2024.e33441

Al-Lhaibi, S. A. and Al-Shabander, B. M., Study the effect of ZnO nanoparticles reinforced sawdust /epoxy composites on mechanical properties, *Dig. J. Nanomater. Biostruct.,* 17(3), 851–860(2022). https://doi.org/10.15251/DJNB.2022.173.851

Biswas, B., Hazra, B., Sinha, A. and Majumdar, A., Effect of incorporation of sub-micronic zirconia particles on the mechanical and thermal behaviour of alkali-treated jute fibre-reinforced epoxy composites, *Mater. Sci. Technol.,* xxxx, 02670836251340767(2025). https://doi.org/10.1177/02670836251340767

Biswas, B., Sawai, P., Santra, A., Gain, A., Saha, P., Mitra, B. C., Bandyopadhyay, N. R. and Sinha, A., Thermal stability, swelling and degradation behaviour of natural fibre based hybrid polymer composites, *Cellul.,* 26(7), 4445–4461(2019). https://doi.org/10.1007/s10570-019-02383-3

Dejene, B. K. and Gudayu, A. D., Achieving performance and functionality in PLA-based packaging: Insights from hybrid composites with false banana (Enset) fiber and ZnO nanoparticles, *J. Thermoplast. Compos. Mater.,* 38(6), 2138–2168(2025). https://doi.org/10.1177/08927057241288125

Demir, M. E., The effect of filler type (tungsten carbide, zinc oxide) and content on the mechanical and wear behavior of jute/flax reinforced epoxy hybrid composites: Experimental and artificial neural network analysis, *Polym. Compos.,* 46(9), 8700–8719(2025). https://doi.org/10.1002/pc.29879

Edlabadkar, A. P., Madhu, M. C., Arunbharathi, R., Sharma, D., Singh, N., Revathi, R. and Mayakannan, S., Optimization of Mechanical Properties of Cordia dichotoma/Alumina Nanoparticle Reinforced Epoxy Nanocomposites Under Alkali Treatment Using ANN Techniques, *J. Environ. Nanotechnol.,* 14(2), 525–540(2025). https://doi.org/10.13074/jent.2025.06.2521549

Harak, S. S., Krishnaveni, K., Karthick, K., Chinnarasu, K., Prasad, P. V. H., Tonk, A. and Mayakannan, S., Experimental Study on the Mechanical Properties of Hybrid Areca and Abaca Fiber Reinforced Polymer Composites, *J. Environ. Nanotechnol.,* 13(4), 92–101(2024). https://doi.org/10.13074/jent.2024.12.244977

Hossain, M. J., Ghosh, R. K., Das, A. K., Nath, S. C., Islam, M. R., Akhter, S. and Rahman, M. S., Investigation of the chemical profiles of seven wood species for their potential applications, *Wood Mater. Sci. Eng.,* 18(2), 650–655(2023). https://doi.org/10.1080/17480272.2022.2058413

Kovačević, Z., Pilipović, A., Meheš, M. and Bischof, S., Zero Waste Concept in Production of PLA Biocomposites Reinforced with Fibers Derived from Wild Plant (Spartium junceum L.) and Energy Crop (Sida hermaphrodita (L.) Rusby), *Polym.,* 17(2), 235(2025). https://doi.org/10.3390/polym17020235

Meravi, M. K. and Panchore, V., Tribological and mechanical characteristics of glass/flax fiber-ZnO reinforced epoxy hybrid composite, *Colloid Polym. Sci.,* 303(3), 411–426(2025). https://doi.org/10.1007/s00396-024-05356-6

Parthasarathy, C., Mayandi, K., Karthikeyan, S. and Senthilrajan, S., Investigation of Snake Grass/Casuarina/Cork Filler Reinforced Bio Polymer Hybrid Composite, *J. Environ. Nanotechnol.,* 13(3), 140–144(2024). https://doi.org/10.13074/jent.2024.09.242711

Prasob, P. A. and Sasikumar, M., Static and dynamic behavior of jute/epoxy composites with ZnO and TiO2 fillers at different temperature conditions, *Polym. Test.,* 69, 52–62(2018). https://doi.org/10.1016/j.polymertesting.2018.04.040

Ru, S., Yang, R., Li, X. and Yang, S., Effect of the Interfacial Bonding Performance Between Coir Fiber and Epoxy Resin Matrix by Adding Adhesive Layer, *Fibers Polym.,* 25(8), 3135–3150(2024). https://doi.org/10.1007/s12221-024-00640-2

Sampathkumar, D., Mohankumar, A., Kulandaivel, A. and Packkirisamy, V., Experimental Investigation on the Micro Structural and Flame Retardant Properties of Various Natural Fiber Reinforced Composites, *J. Nat. Fibers.,* 21(1), 2341125(2024). https://doi.org/10.1080/15440478.2024.2341125

Kumar, R. S., Devi, V. V., Nivedhitha, D. M., Satya, S. S., Visakan, S., Sharma, S. B. and Kumar, S. B. S., Effect of nanoparticles in natural fiber reinforced polymer composite, *Mater. Today: Proc.,* S2214785323020266(2023). https://doi.org/10.1016/j.matpr.2023.04.130

Sbardella, F., Rivilla, I., Bavasso, I., Russo, P., Vitiello, L., Tirillò, J. and Sarasini, F., Zinc oxide nanostructures and stearic acid as surface modifiers for flax fabrics in polylactic acid biocomposites, *Int. J. Biol. Macromol.,* 177, 495–504(2021). https://doi.org/10.1016/j.ijbiomac.2021.02.171

Senniangiri, N., Gokulkannan, S., Kumar, S. D. and Gokul, S., Enhancing Mechanical, Moisture Resistance, and Fire-retardant Properties of Nelumbo nucifera Fiber/Epoxy Nanocomposites with Zinc Oxide Nanoparticles, *J. Environ. Nanotechnol.,* 14(1), 253–265(2025). https://doi.org/10.13074/jent.2025.03.2511215

Shanti, Y., Vemula, J. and Satyadevi, A., Effect of combined natural and synthetic filler addition on the behaviour of glass fibre reinforced composite, *Adv. Mater. Process. Technol.,* 10(3), 1784–1799(2024). https://doi.org/10.1080/2374068X.2023.2201750

Siddiqui, M. A. S., Rabbi, M. S. and Rahman, M. T., An experimental review on enhancing the low and high-velocity impact resistance of NFCs through nanoparticle reinforcement, *J. Reinf. Plast. Compos.,* 44(17-18), 1270-1298(2025). https://doi.org/10.1177/07316844241240569

Suja, R. N., Sridevi, B. and Thiagamani, S. M. K., Mechanical and Dynamic Mechanical Characterization of Epoxy Composites Reinforced with Casuarina Leaf Bio Fibre, *J. Res. Updates Polym. Sci.,* 13, 66–74(2024). https://doi.org/10.6000/1929-5995.2024.13.08

Tasnim, T., Rabbi, M. S., Adil, M. M. and Hasib, M. A., An experimental study on jute/banana fiber reinforced poly(vinyl alcohol) composites with nanofiller, *J. Vinyl Add. Tech.,* 30(5), 1327–1340(2024). https://doi.org/10.1002/vnl.22127

Thandavamoorthy, R., Mohanavel, V., Sivapragasam, A., Vekariya, V., Paul, D., Velmurugan, P., Al Obaid, S., Alharbi, S. A. and Basavegowda, N., Environmental sustainability and waste conversion of Prosopis juliflora fibre-reinforced ZnO nanofiller particulates PLA composite- mechanical and thermal analysis, *Heliyon.,* 10(19), e38327(2024). https://doi.org/10.1016/j.heliyon.2024.e38327

Tumusiime, G., Wambua, P., Rwahwire, S., Njuguna, D. and Yiga, V. A., Production and mechanical characterization of reinforced zinc oxide nanoparticle-coated silk waste bio-composites, *Polym. Bull.,* 80(8), 8799–8818(2023). https://doi.org/10.1007/s00289-022-04475-w

Zaman, S. U., Shahid, S., Shaker, K., Nawab, Y., Ahmad, S., Umair, M., Khaliq, Z. and Azam, F., Development and characterization of chemical and fire resistant jute/unsaturated polyester composites, *J. Text. Inst.,* 113(3), 484–493(2022). https://doi.org/10.1080/00405000.2021.1889131

Wu, Y., Cai, L., Mei, C., Lam, S. S., Sonne, C., Shi, S. Q. and Xia, C., Development and evaluation of zinc oxide-blended kenaf fiber biocomposite for automotive applications, *Mater. Today Commun.,* 24, 101008(2020). https://doi.org/10.1016/j.mtcomm.2020.101008

Yang, Y., Nie, W., Zhang, H., Yu, T., Wu, K., Wang, J., Cui, Y. and Pan, L., Homogeneous and aligned ZnO nanorods@Jute fibers for enhanced mechanical/microwave absorbing performance and thermal stability, *Mater. Chem. Phys.,* 295, 127031(2023). https://doi.org/10.1016/j.matchemphys.2022.127031

Yang, Y., Zhang, H., Liu, X., Deng, Y., Sun, M., Wang, J., Cui, Y., Pan, L. and Chen, Z., Hierarchical interface design of jute fibers/polypropylene composites for enhanced interfacial and mechanical properties, *J. Cleaner Prod.,* 450, 141966(2024). https://doi.org/10.1016/j.jclepro.2024.141966